Virology 422 (2012) 214–223

Contents lists available at SciVerse ScienceDirect

Virology

journal homepage: www.elsevier.com/locate/yviro

The N-terminal helix α_0 of hepatitis C virus NS3 protein dictates the subcellular localization and stability of NS3/NS4A complex

Ying He [a], Leiyun Weng [b], Rui Li [a], Li Li [a], Tetsuya Toyoda [b], Jin Zhong [a,*]

[a] Unit of Viral Hepatitis, Key Laboratory of Molecular Virology and Immunology, Institut Pasteur of Shanghai, Shanghai Institutes for Biological Sciences, Chinese Academy of Science, Shanghai, 200025, China

[b] Units of Viral Genome Regulation, Key Laboratory of Molecular Virology and Immunology, Institut Pasteur of Shanghai, Shanghai Institutes for Biological Sciences, Chinese Academy of Science, Shanghai, 200025, China

ARTICLE INFO

Article history:
Received 21 October 2011
Accepted 22 October 2011
Available online 14 November 2011

Keywords:
HCV
NS3
Helix α_0
Membrane association
Protein degradation

ABSTRACT

The N-terminal amphipathic helix α_0 of hepatitis C virus (HCV) NS3 protein is an essential structural determinant for the protein membrane association. Here, we performed functional analysis to probe the role of this helix α_0 in the HCV life cycle. A point mutation M21P in this region that destroyed the helix formation disrupted the membrane association of NS3 protein and completely abolished HCV replication. Mechanistically the mutation did not affect either protease or helicase/NTPase activities of NS3, but significantly reduced the stability of NS3 protein. Furthermore, the membrane association and stability of NS3 protein can be restored by replacing the helix α_0 with an amphipathic helix of the HCV NS5A protein. In summary, our data demonstrated that the amphipathic helix α_0 of NS3 protein determines the proper membrane association of NS3, and this subcellular localization dictates the functional role of NS3 in the HCV life cycle.

Introduction

Hepatitis C virus (HCV) is the member of the distinct *Hepacivirus* genus in *Flaviviridae* family. Its infections are often persistent and lead to chronic hepatitis, which can develop into liver cirrhosis, and hepatocellular carcinoma. Currently, over 170 million people worldwide are infected with HCV. The standard of care is the combination therapy of interferon-*a* (IFN-*a*) and ribavirin, however, the effectiveness of this treatment is insufficient especially for the patients infected with HCV of genotype I.

HCV contains a 9.6-kb positive single-stranded RNA genome that encodes a polyprotein precursor of about 3000 amino acids flanked by 5′- and 3′-UTR regions that are important for translation and replication of the viral RNA (Moradpour et al., 2002; Takamizawa et al., 1991). The polyprotein precursor is co- and post-translationally processed by cellular and viral proteases to yield mature structural (Core, E1, E2) and nonstructural proteins (p7, NS2, NS3, NS4A, NS4B, NS5A and NS5B) (Hijikata et al., 1991, 1993; Reed and Rice, 1998; Shimotohno et al., 1995). NS3 is a bifunctional molecule with an N-terminal serine protease domain which, together with the NS4A cofactor, is essential for cleavage at NS3/4A, NS4A/4B, NS4B/5A and NS5A/5B sites, and a C-terminal domain functioning as an RNA helicase/NTPase (Bartenschlager et al., 1993; Eckart et al., 1993; Grakoui et al., 1993b; Kim et al., 1995). In addition, NS3 is the cofactor of NS2 cysteine autoprotease responsible for cleavage at NS2/NS3 site. Both enzyme activities have been well characterized, and high-resolution structures have been solved. The serine protease domain adopts a chymotrypsin-like fold with residues H57, D81 and S139 forming its catalytic triad (Kim et al., 1996). The NS3 helicase unwinds RNA and DNA homoduplexes and heteroduplexes in a 3′ to 5′ direction (Kim et al., 1995).

Formation of a membrane-associated replication complex, composed of viral proteins, replicating viral RNA, and altered cellular membranes, is a hallmark of all plus-strand RNA viruses including HCV. HCV RNA replication occurs in association with altered cytoplasmic membranes which are termed as “membranous web” (Egger et al., 2002; Moradpour et al., 2003). NS4B is sufficient to induce the membranous web formation and has been proposed to serve as a scaffold for replication complex assembly. NS5B, the RNA-dependent-RNA polymerase, is an essential component of this RNA replication machinery (Lohmann et al., 1997). Almost all the HCV nonstructural proteins have been studied for structural determinants of membrane association. The N-terminal domain of NS4A is predicted to form a transmembrane α-helix involved in membrane anchorage of the NS3-4A complex (Brass et al., 2008; Gosert et al., 2005). Moradpour et al. (Gouttenoire et al., 2009b) reported that an amphipathic α-helix at the C terminus of NS4B (amino acid residues 229 to 253) was essential for membrane association and was involved in the formation of a functional HCV replication complex. In addition, an amphipathic α-helix extending from amino acids 5 to 25 of the N-terminus of NS5A was identified as a membrane anchor domain by NMR spectroscopy (Penin et al., 2004). For NS3, the amphipathic

* Corresponding author at: Institut Pasteur of Shanghai, Chinese Academy of Science, 225 South Chongqing Road, Shanghai, 200025, China. Fax: +86 21 63859365.
E-mail address: jzhong@sibs.ac.cn (J. Zhong).

0042-6822/$ – see front matter © 2011 Elsevier Inc. All rights reserved.
doi:10.1016/j.virol.2011.10.021

helix α_0, formed by the N-terminal amino acid residues 12–23 highly conserved among HCV genotypes, was reported to serve as an essential structural determinant for the membrane association of the NS3-NS4A complex. However, the detailed virological and biological functions of this amphipathic helix in the HCV life cycle have not been fully explored.

Here we analyzed the detailed functions of the amphipathic helix α_0 of NS3 in the HCV life cycle. We demonstrated that the helix α_0 served as the primary structural determinant for the membrane association of NS3 and NS3/4A protease complex, and this subcellular localization prevented the degradation of the NS3 protein.

Results

M21P mutation destroyed the N-terminal amphipathic α helix of NS3 protein

A previous study demonstrated that the N-terminal 10–24 residues of HCV NS3 protein formed an amphipathic helix α_0, a critical determinant for ER membrane association of NS3-NS4A complex (Brass et al., 2008). However, the biological function of this α helix in HCV life cycle has not been fully explored. We engineered a point mutation (M21P) from methionine to proline at amino acid 21 of NS3 of JFH1, a genotype 2a HCV strain (Fig. 1A). Secondary structure prediction analysis indicated that the M21P mutation impaired the helix structure formation, as the predicted overall 22% helix content for the wild-type decreased to 11% for the mutant peptide (Fig. 1B). This prediction was further confirmed by circular dichroism analysis of the peptides covering the N-terminal 10–24 amino acids of JFH1 NS3 protein. As shown in Fig. 1C, the wild-type peptide displayed a typical alpha helix absorption curve, while the M21P peptide did not. These results demonstrated that the M21P mutation destroyed the N-terminal amphipathic alpha helix of NS3.

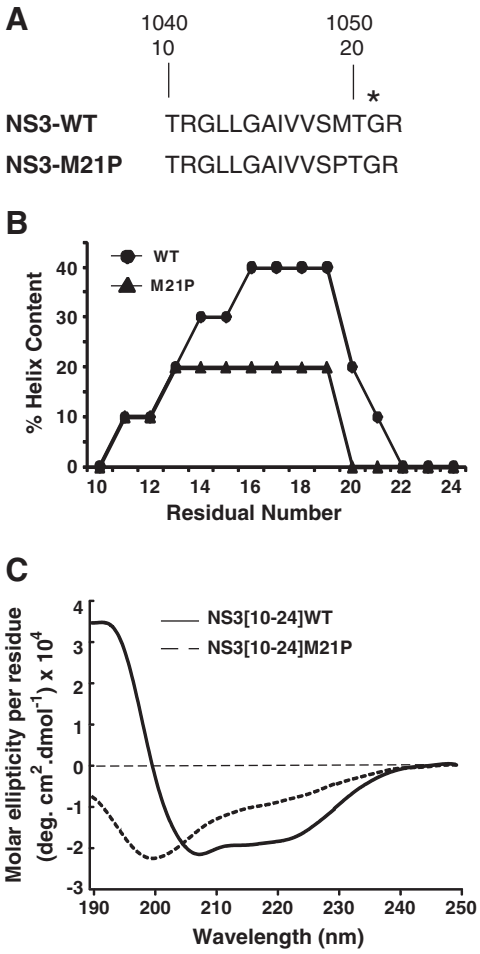

Fig. 1. M21P destroyed the N-terminal amphipathic helix α_0 of NS3. A. Schematic representation of amino acids 10–24 of wild-type and M21P mutant NS3 protein (JFH1 strain). The point mutation at position 21 is indicated by the asterisk. Nucleotides (1040–1050) and amino acids (10–20) are numbered according to the HCV polyprotein and NS3 respectively. B. Prediction of the secondary structure of amino acids 10–24 segment of NS3 using Agadir software (http://agadir.crg.es/) (Munoz and Serrano, 1994) for the helix contents. C. Circular dichroism analysis of peptides encompassing the amino acids 10–24 of wild-type and M21P mutant NS3 proteins.

Disruption of the helix α_0 did not affect NS3 helicase/NTPase activities

HCV NS3 protein is a multifunctional protein with helicase and NTPase activities in the C-terminal two-thirds. Therefore, we examined whether disruption of α_0 at the N-terminus affected the helicase/NTP activities. We expressed and purified His-tagged wild-type and M21P mutant recombinant NS3 proteins. All recombinant NS3 proteins were purified to greater than 95% purity (Fig. 2A). Next we examined the helicase and NTPase activities of recombinant NS3 proteins using the previously reported assays (Zhang et al., 2005). For the helicase assay, a synthetic 30-nucleotide 5′-end ^{32}P-radiolabeled oligonucleotide was annealed to a 54-nucleotide single-stranded DNA to form a partially duplex DNA substrate with 5′ and 3′ overhanging ends. Upon unwinding by NS3 helicase, the 30-nucleotide labeled DNA strand was released and trapped by a complementary capture strand to form a duplex. As shown in Fig. 2B, both the wild-type and M21P NS3 proteins efficiently unwound the DNA duplex substrate in a dose-dependent manner. Similarly, for the NTPase assay, the wild-type and M21P NS3 proteins hydrolyzed γ-^{32}P GTP with comparable efficiencies (Fig. 2C). These results demonstrated that the M21P mutation did not affect the helicase or NTPase activities of NS3.

Disruption of the helix α_0 abolished HCV replication

To determine the functional role of the NS3 helix α_0 in HCV life cycle, the M21P mutation was introduced into pSGR-luc-JFH1, a bi-cistronic subgenomic replicon that expressed firefly luciferase, for direct detection of luciferase as a measurement of HCV RNA replication capacity (Targett-Adams and McLauchlan, 2005). Wild-type, M21P mutant and NS5B polymerase defective GND mutant (Wakita et al., 2005) *in vitro* transcribed replicon RNAs were electroporated into Huh7 cells, and luciferase activities were measured at 4, 24 and 48 h post-electroporation. As shown in Fig. 3A, the luciferase activity of the wild-type replicon increased about 30-fold after 48 h of electroporation, whereas the luciferase activity of the M21P and GND replicons declined below the basal levels after 4 h, indicating the M21P mutation abolished the HCV RNA replication.

Next, we used the infectious HCVcc system (Lindenbach et al., 2005; Wakita et al., 2005; Zhong et al., 2005) to examine the effect of the M21P mutation on HCV life cycle. Wild-type and M21P mutant JFH1 genomic RNAs were electroporated into Huh7.5.1 cells. Consistent with the results of subgenomic replicon transfection, M21P mutant JFH1 RNA did not produce infectious viruses, whereas wild type displayed viral expansion kinetics as previously described (Zhong et al., 2005), with extracellular infectivity titers peaking at 1500 ffu/ml on day 21 post-electroporation (Fig. 3B). Furthermore, immunofluorescent staining of HCV E2 proteins indicated that cells transfected with M21P mutant remained negative throughout the entire experiment (Fig. 3C), strongly suggesting that the M21P mutation completely abolished HCV replication.

Next, we examined the effects of the M21P mutation on HCV non-structural protein expression. Plasmids that contain wild-type, M21P, a NS3 protease-defective mutant H57A (Bartenschlager et al.,

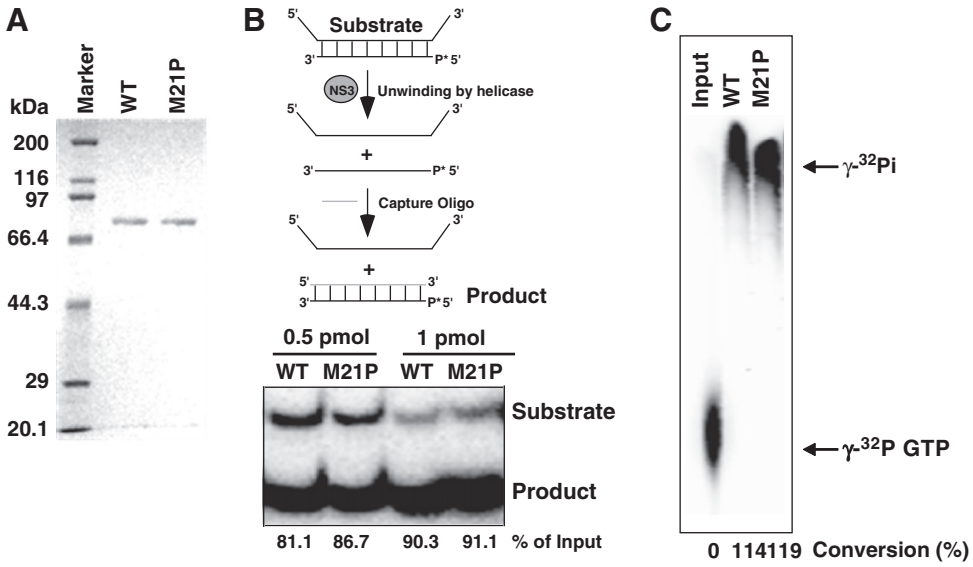

Fig. 2. Disruption of helix α_0 did not affect the NTPase/helicase activity of NS3. A. SDS-PAGE analysis of purified recombinant wild-type and M21P NS3 proteins. Ten picomoles of each protein were loaded onto 10% SDS-PAGE gels and visualized by Coomassie blue staining. Molecular mass markers are on the left. B. Helicase activity of wild-type and M21P mutant NS3 proteins. Helicase activity was measured with a radio-labeled double-stranded DNA substrate unwound by 0.5 or 1 pmole of wild-type and M21P mutant NS3 proteins, and quantified with a PhosphorImager. The percentage of input, calculated as the ratio of the product over the total input (substrate + product), was indicated at the bottom. Schematic representation of the assay is shown on the top. C. NTPase activity of wild-type and M21P mutant NS3 proteins. 5 pmol [γ-^{32}P] GTP was incubated with an aliquot of 5 pmol NS3 proteins at 37 °C for 30 min and the radioactive phosphate product was separated by the thin-layer chromatography and quantified with a PhosphorImager. The NTPase activity expressed as the percentage of radioactive phosphate converted from input [γ-^{32}P] GTP was indicated at the bottom.

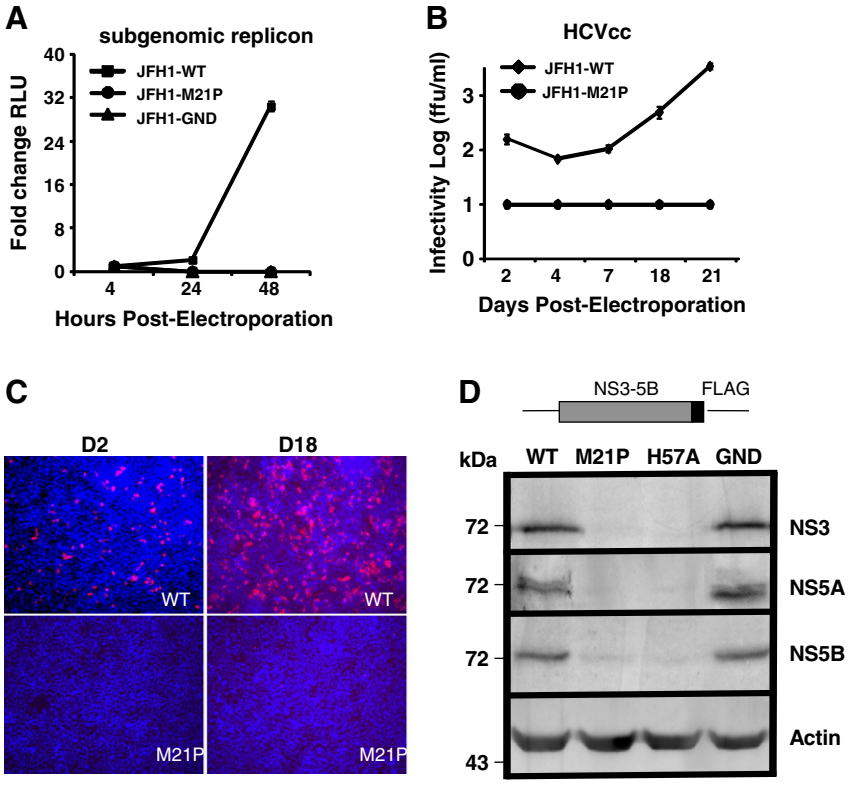

Fig. 3. Disruption of helix α_0 abolished HCV replication and virus production A. The luciferase activity of JFH1 subgenomic replicon expressing the wild type, M21P or GND. The subgenomic luciferase reporter replicon is a bicistronic RNA containing firefly luciferase expressed via the HCV's IRES and NS3-5B proteins expressed via the EMCV's IRES (Lohmann et al., 1999). The *in vitro* transcribed replicon RNA was electroporated into Huh7.5.1 cells and the luciferase activities were measured at the indicated times. The error bars were calculated from 4 independent experiments. B. The supernatant infectivity titers of JFH1 HCVcc containing the wild-type or M21P mutant NS3. The *in vitro* transcribed full-length genomic JFH1 RNA containing the wild-type or M21P mutant NS3 were electroporated into Huh7.5.1 cells, and the culture supernatants were harvested at the indicated times post-electroporation, and determined for the infectivity titers. The error bars were calculated from 3 independent experiments. C. The E2 immunostaining of Huh7.5.1 cells at day 2 and 18 post-electroporation. E2 staining was in red and nuclei were stained with Hoechst (blue). D. Western blot analysis of HCV non-structural protein expression. Plasmids expressing the wild-type, M21P, H57A or GND of JFH1 NS3-NS5B were transfected into Huh7.5.1 cells, and the cell lysates were collected at day 2 post-transfection for western blot. Expressions of HCV NS3 (72 kDa), NS5A (two bands corresponding to p56 and p58, around 72 kDa), NS5B-FLAG (72 kDa) and actin (45 kDa) are shown from top to bottom.

1993; Grakoui et al., 1993a), and GND mutant of the NS3-NS5B encoding region were transfected into Huh7.5.1 cells, and the NS3, NS5A and NS5B protein levels were determined at day 2 post-transfection. As shown in Fig. 3D, NS3, NS5A and NS5B protein levels were dramatically decreased for M21P and H57A compared to wild-type and GND mutant. Since the maturation of NS5A and NS5B proteins is carried out by the NS3/NS4A serine protease, the decreased NS5A and NS5B levels of M21P mutant were likely caused by insufficient NS3 protein level. Altogether, these data suggested that the disruption of N-terminal helix α_0 of NS3 protein reduced NS3 protein levels and abolished HCV replication.

Disruption the helix α_0 led to NS3 degradation

The reduced NS3 protein level of M21P mutant could be because cleavage between NS2 and NS3 or NS3 and NS4A was affected by the M21P mutation, or the M21P NS3 protein was unstable. We tested each of these possibilities.

Because the autoprotease activity of NS2 requires both NS2 and the N-terminal 181 amino acids of NS3 (Grakoui et al., 1993b; Schregel et al., 2009), we first investigated whether the M21P mutation in the N-terminus of NS3 affected NS2 protease activity. Plasmids expressing N-terminal HA-tagged NS2 protein fused with the wild-type, M21P, H57A NS3 were transfected into Huh7.5.1 cells. Cell lysates were collected at 48 h post-transfection and analyzed by western blot. As shown in Fig. 4A, the HA-NS2 expression levels were comparable among the wild type and mutants, whereas the NS3 levels were significantly reduced in the M21P mutant, suggesting that cleavage at the NS2 and NS3 junction was not affected by the M21P mutation in NS3.

Next, we examined whether the M21P mutation affected cleavage at the NS3/NS4A junction. Plasmids that expressed the wild-type, M21P, or H57A mutant NS3 protein fused with a C-terminal FLAG-tagged NS4A were transfected into Huh7.5.1 cells. Cell lysates were collected at 48 h post-transfection and analyzed by western blot. As shown in Fig. 4B, both NS3 and FLAG-tagged NS4A proteins were detected for the wild type, indicative of efficient cleavage between NS3 and NS4A. In contrast, for the protease-defective H57A construct, neither NS3 nor NS4A was detected, and uncleaved NS3/NS4A protein was detected by both anti-NS3 and anti-Flag antibodies. Interestingly, for the M21P mutant, NS3 protein was barely detected although mature NS4A was detected with no uncleaved NS3/NS4A product. These results suggested that the cleavage at the NS3/4A junction by NS3 protein was not affected by the M21P mutation. Instead, this mutation may possibly affect NS3 stability, and decreased level of mature NS4A in the M21P mutant construct may reflect the instability of NS3/NS4A precursor.

To evaluate the effect of the M21P mutation on the stability of NS3 protein, we transfected plasmids expressing wild-type, M21P, or H57A NS3-NS4A proteins into Huh7.5.1 cells, and added proteasomal inhibitor MG132 on day 1 post-transfection to inhibit protein degradation. Cell lysates were collected 48 h later, and analyzed by western blot. As shown in Fig. 4C, the M21P NS3 expression level was much lower than the wild-type and H57A NS3. However, in the presence of MG132, the M21P NS3 protein level increased about 3.52-fold whereas the wild-type increased only 1.26-fold and H57A NS3 increased 1.54-fold, indicating that the M21P NS3 protein was more prone to degradation. The restoration of mature M21P NS3 protein level by the proteasomal inhibitor also suggested that the M21P mutation did not impair the NS3 protease activity catalyzing the NS3-NS4A cleavage. We noted that a larger band appeared above the wild-type and M21P NS3 protein in the presence of MG132, and this band likely represented the uncleaved NS3-4A precursor possibly due to the influence of MG132 on the NS3 protease activity.

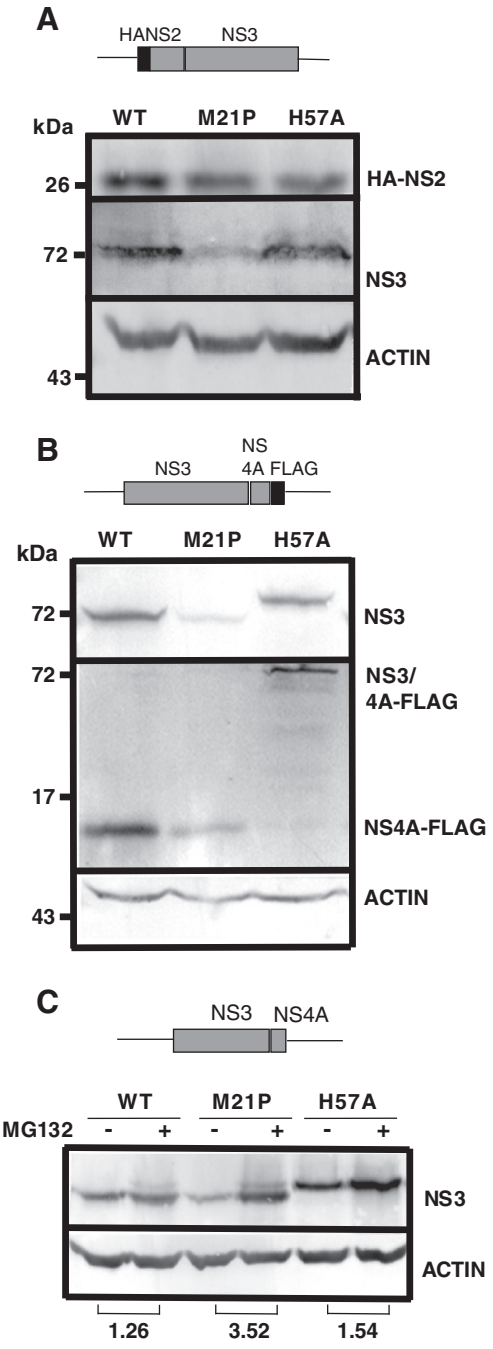

Fig. 4. Disruption of helix α_0 reduced the stability of NS3 protein. A. Western blot analysis of NS2 and NS3 proteins. The plasmids expressing HA-tagged NS2 fused with wild-type, M21P or H57A NS3 were transfected into Huh7.5.1 cells, and the cell lysates were collected at 48 h post transfection and analyzed by western blot using antibodies specific for HA or NS3. B. Western blot of NS3 and NS4A proteins. The plasmids expressing wild-type, M21P or H57A NS3 fused with FLAG-tagged NS4A were transfected into Huh7.5.1 cells, and the cell lysates were collected at 48 h post transfection and analyzed by western blot using antibodies specific for NS3 or FLAG. C. Western blot of NS3 with or without MG132 treatment. Huh7.5.1 cells were transfected with the plasmids expressing wild-type, M21P or H57A NS3 fused with NS4A for 24 h, and then treated with 5 μM MG132 (sigma) for 16 h. The cell lysates were analyzed by western blot. The relative expression levels of NS3 proteins were quantified by ImageJ and the fold-change of NS3 protein levels are indicated at the bottom. Actin was used as the internal control in all experiments.

Taken together, these results demonstrated that disruption of the amphipathic helix α_0 of NS3 protein did not affect cleavage at the NS2/3 and the NS3/4A junctions but significantly reduced NS3 stability.

Membrane association of NS3 determined by helix α_0 accounted for NS3 stability

A previous study showed that the amphipathic helix α_0 was an important structural determinant for NS3 membrane association (Brass et al., 2008), therefore, we hypothesized that the disruption of the NS3 helix α_0 by the M21P mutation resulted in disassociation of NS3 protein from membrane, and that cytosolic NS3 was prone to degradation. To test this hypothesis, we transfected plasmids expressing GFP fused at the N-terminus to a peptide of 10–24 amino acids of wild-type or M21P NS3, and analyzed the GFP subcellular localization by confocal microscopy. As shown in Fig. 5A, $NS3_{10-24wt}$-GFP displayed

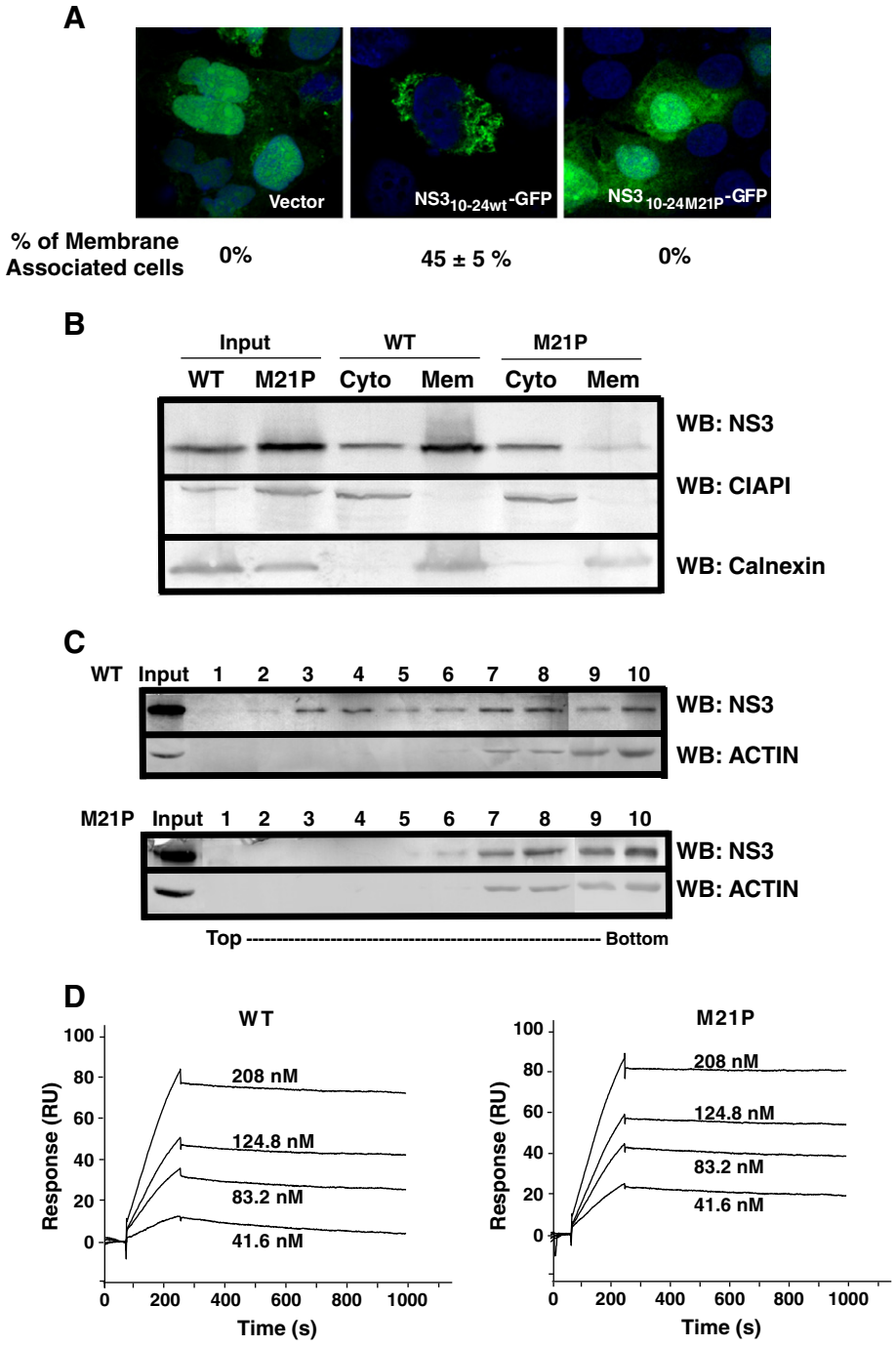

Fig. 5. Helix α_0 determined subcellular localization of NS3. A. Subcellular localization of helix α_0 fused GFP. Huh 7 cells were transfected with vector GFP-N1, $NS3_{10-24wt}$-GFP, or $NS3_{10-24M21P}$-GFP and after 48 h, GFP fluorescence was examined by fluorescence microscopy. Percentage of membrane-associated cells was calculated from about 300 GFP-positive cells in each fluorescence image, and the standard deviation was calculated from 5 randomly selected images. B. Western blot analysis of NS3 proteins in the cytosolic and membrane fractions. The Huh7.5.1 cells expressing the wild-type or M21P NS3-NS4A (5 μM MG132 treated) were subjected for the separation of cytosolic and membrane fractions as described in the Methods. The total cell lysates and each fraction were analyzed by western blot. cIAPI, a cytosolic protein, and calnexin, an ER protein, were included as the marker for the cytosolic and membrane fractions respectively. C. Membrane floatation of NS3 analyzed by western blot. U2-OS cells were transfected with plasmids expressing the wild-type or M21P NS3-NS4A, and then treated with 5 μM MG132. Membrane floatation gradient centrifugation was performed as described in the Methods. Ten fractions were collected from the top and analyzed by western blot. D. Biacore analysis of the NS3 and NS4A interaction. Biotin labeled NS4A was immobilized to the chip and various concentrations of recombinant wild-type and M21P mutant NS3 proteins were injected as analyte through the reference and NS4A-coupled surfaces. Sensorgrams were analyzed using a 1:1 binding model.

a punctuate, membrane-associated fluorescence pattern in roughly 45% of GFP-positive cells, whereas the fluorescence of $NS3_{10-24M21P}$-GFP was diffuse through the cytoplasm and nucleus, similar to the vector control.

To confirm the localization difference between wild-type and M21P NS3, we transfected plasmids expressing wild-type or M21P mutant NS3-4A into Huh7.5.1 cells and MG132 was added to the M21P mutant transfected cells for inhibition of its degradation. Cell lysates were fractionated and subjected to western blot using calnexin, a known ER transmembrane protein, as a marker for the membrane fraction and the cytosol-localized inhibitor of apoptosis protein cIAP-1 for the cytosolic fraction. As shown in Fig. 5B, the wild-type NS3 protein was mainly localized in the membrane fraction with only a small amount in the cytosolic fraction, whereas the majority of M21P mutant NS3 protein was recovered in the cytosolic fraction. This result was further confirmed by a membrane floatation assay in which the wild-type NS3 proteins were distributed to a wider range of fractions whereas the M21P NS3 proteins were mostly distributed to the bottom fractions (Fig. 5C). Altogether, these results demonstrated that NS3-M21P lost the ability to associate with the membrane.

Previous work demonstrated that the N-terminal 22 amino acids of NS3 were important for interaction of NS3 with NS4A (Failla et al., 1995), and NS4A increased the stability of NS3 (Satoh et al., 1995), raising a possibility that the M21P mutation may destabilize NS3 by disrupting the NS3-NS4A interaction. To test this possibility, we used the *in vitro* Biacore assay to examine the NS3 and NS4A interaction, using purified recombinant NS3 proteins (Fig. 2A) and *in vitro* synthesized NS4A peptide. The interaction between NS3 and NS4A was analyzed with NS4A coupled to the chip by biotin labeled at its C-terminus and NS3 injected as the analyte in a serial dilution. As shown in Fig. 5D, the binding of wild-type and M21P mutant NS3 to NS4A appeared similar. In addition, when the sensorgrams were analyzed by a 1:1 binding model, global fitting revealed that the affinity of NS3 wild-type to NS4A was $K_{DWT}=7.76$ nM and the M21P mutant to NS4A was $K_{DM21P}=4.16$ nM. The association rate constant of M21P ($k_{onm21p}=14600\ M^{-1}\ s^{-1}$) was slightly higher than wild-type ($k_{onwt}=9763\ M^{-1}\ s^{-1}$) and the dissociation rate constant of M21P ($k_{offm21p}=0.000061\ s^{-1}$) was similar to wild-type ($k_{offwt}=0.000076\ s^{-1}$). All these results demonstrated that the disruption of the NS3 helix α_0 did not affect the physical binding of NS3 to NS4A.

Restoration of NS3 membrane association rescued its stability

Next we tested whether the restoration of membrane association of NS3 protein could rescue the stability of the NS3 protein. It has been reported that amino acids 5 to 25 of the N-terminus of HCV NS5A protein also form a well-defined amphipathic alpha helix allowing for the membrane association of NS5A (Penin et al., 2004). Therefore, we replaced NS3 helix α_0 with the JFH1 NS5A amphipathic helix (Fig. 6A). As shown in Fig. 6B, the NS3 expression level of the NS3-NS5Ahelix was comparable to that of wild type and higher than that of M21P mutant. Furthermore, the fractionation analysis showed that the NS3 protein of the NS3-NS5Ahelix was mainly located in the membrane fraction, similar to wild-type, indicating that restoration of NS3 membrane localization could restore its stability (Fig. 6C).

Next we investigated whether the replacement of NS3 helix α_0 with the NS5A amphipathic helix could further rescue HCV replication. We introduced the NS5A helix sequence into the NS3 helix α_0 region of Rz-JFH-1, a previously reported plasmid-based system with the full-length JFH1 cDNA flanked by two self-cleaving ribozymes to produce HCVcc upon plasmid transfection (Kato et al., 2007) and transfected into Huh7.5.1 cells. As shown in Fig. 6D, almost no mature NS3 protein was detected in the Rz-NS5Ahelix transfected cells. Since cleavage between the NS3-5Ahelix and 4A was intact and the cleaved NS3 was stable, we hypothesized that cleavage at the NS2 and NS3 junction was affected by the heterologous replacement. To test this hypothesis, we engineered the NS5A helix into the HA-NS2-3 construct and transfected into Huh7.5.1 cells. As shown in Fig. 6E, no cleaved NS2 or NS3 was detected in the HA-NS2-3-NS5A helix-transfected cells, suggesting although the NS5A amphipathic helix could restore the NS3 subcellular localization but disrupt the NS2-3 cleavage, thereby impairing HCV replication.

Next we examined whether NS3-5Ahelix affected the replication of an HCV subgenomic replicon. The *in vitro* synthesized HCV bi-cistronic subgenomic RNA expressing firefly luciferase was electroporated into Huh7 cells, and luciferase activities were measured at 4, 24 and 48 h post-transfection using the same assay described in Fig. 3A. As shown in Fig. 6F, replacement of NS3 helix α_0 with NS5A helix failed to rescue HCV RNA replication despite that it could restore the membrane association and protein level of NS3, suggesting that NS3 helix α_0 may contribute to HCV replication by more than dictating the subcellular localization and promoting stability of NS3 protein.

Finally, we investigated whether the replacement of the JFH1 NS3 helix α_0 with the same segment of different HCV genotypes could restore NS3 membrane localization, stability and HCV replication. As shown in Fig. 7A, the sequence of NS3 helix α_0 is highly conserved, only varying at positions 13, 16, 18, 19 and 21 among H77C (genotype 1a), Con1 (genotype 1b), SA13 (genotype 5a) and JFH1. We replaced the NS3 helix α_0 in Rz-JFH-1 construct with the same segment of H77C (identical to Con1) or SA 13 and transfected into Huh7.5.1 cells. As shown in Fig. 7B, at 48 h post-transfection, HCV core, NS3 and NS5A displayed comparable expression levels in Rz-H77C, Rz-SA13, and Rz-JFH1 transfected cells. Furthermore, both Rz-NS3-H77Chelix and Rz-NS3-SA13helix displayed comparable amounts of HCV-positive cells to wild-type on day 6 post transfection while Rz-NS3-M21P showed no HCV-positive cells (Fig. 7C). This clearly demonstrated that NS3 stability and HCV replication capability were restored by homologous replacement of the JFH1-NS3helix with H77C or SA13 NS3 helix α_0.

Discussion

Eukaryotic intracellular membrane organelles are highly organized structures and provide essential places for occurrence of numerous biological events. Many intracellular pathogens such as viruses have evolved to utilize these membrane structures for their own survival. HCV replication occurs in a membrane-derived replication complex consisting of viral genome and nonstructural proteins that require correct subcellular localization for their functions in the viral life cycle. The previously identified N-terminal amphipathic helix α_0 of HCV NS3 protein was an important structural determinant for NS3 membrane association (Brass et al., 2008). Here we demonstrated that impaired membrane association of NS3 by a point mutation (M21P) or the deletion of the entire helix α_0 (data not shown) reduced the stability of NS3 protein, while had no effect on the protease and helicase/NTPase activities of NS3, proteolytic cleavages at NS2/NS3 and NS3/NS4A sites, or the interaction between NS3 and NS4A. When the helix α_0 was replaced with an amphipathic helix derived from HCV NS5A protein, the membrane association and stability of NS3 protein were both restored. Furthermore, inhibition of cellular proteasome could restore the NS3 stability, but not the membrane association (Fig. 5B). From these data we concluded that the helix α_0 allowed the NS3-NS4A precursor or the mature NS3 protein to associate with the membrane, which avoided protein degradation by the cellular degradation machinery. Therefore, the helix α_0 was not only the determinant for the subcellular localization of NS3, but also the determinant for the protein stability.

A previous study showed that NS4A, the cofactor of NS3 serine protease, could help NS3 localize to membrane and stabilize NS3 protein (Tanji et al., 1995). In our study, we found that the disruption of the helix α_0 led to the membrane dissociation and degradation of

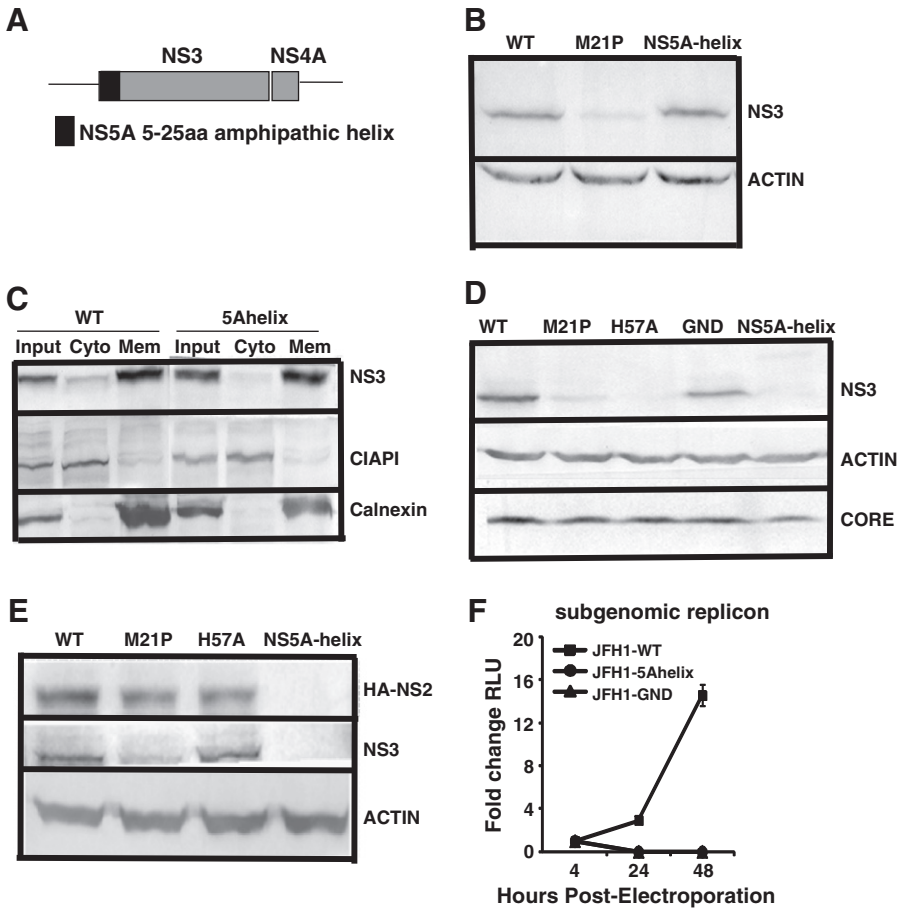

Fig. 6. A NS5A-derived amphipathic α helix could restore NS3 membrane association and its stability. A. Schematic representation of replacement of NS3 helix α_0 with the N-terminal 5–25 amino acids of NS5A amphipathic α helix. B. Western blot analysis of NS3 expression with helix α_0 replaced with the NS5A amphipathic α helix. Huh7.5.1 cells were transfected with plasmids expressing the wild-type, M21P or NS5A-helix chimeric NS3-NS4A proteins, and the cell lysates were collected at day 2 post-transfection and analyzed by western blot. C. Western blot analysis of NS3 proteins in the cytosolic and membrane fractions. The Huh7.5.1 cells expressing the wild-type or NS5A-helix fused NS3 proteins were subjected for the separation of cytosolic and membrane fractions. The total cell lysates and each fraction were analyzed by western blot. cIAPI, a cytosolic protein, and calnexin, an ER protein, were included as the marker for the cytosolic and membrane fractions respectively. D. Western blot analysis of NS3 and core in the cells transfected with the plasmids expressing HCVcc. Rz-JFH1-WT, Rz-JFH1-M21P, Rz-JFH1-H57A, Rz-JFH1-GND, or Rz-JFH1-NS5Ahelix were transfected into Huh7.5.1 cells to examine viral production. At 48 h post transfection, cells lysates were analyzed by western blot for HCV Core and NS3 protein expressions. E. Western blot analysis of HCV NS2 and NS3 proteins. The plasmids expressing HA-tagged NS2 fused with wild-type, M21P, H57A or NS5A-helix chimeric NS3 were transfected into Huh7.5.1 cells, and the cell lysates were collected at 48 h post transfection and analyzed by western blot using antibodies specific for HA or NS3. F. The luciferase activity of JFH1 subgenomic replicon expressing the wild type, 5Ahelix or GND. A representative experiment of three independent repetitions, each measured in duplicate was shown.

NS3 even though it did not affect the NS3-NS4A interaction. This suggested that NS4A alone was not sufficient enough to confer the membrane association and stability of NS3 protein. In fact, the helix α_0 defective NS3-NS4A (M21P) displayed not only the reduced NS3 protein level but also the reduced NS4A protein level (Fig. 4B), likely reflecting the reduced stability of uncleaved NS3-NS4A precursor. On the contrary, the protease defective NS3-NS4A (H57A) displayed high expression level of uncleaved NS3-NS4A precursor despite that it could not produce the mature NS4A cofactor. Therefore, we proposed that the helix α_0 served as the primary structural determinant of uncleaved NS3-4A precursor for its subcellular localization and stability. After the cleavage at the NS3-NS4A site was completed, the N-terminal transmembrane domain of NS4A inserted into the membrane (Brass et al., 2008; Gosert et al., 2005) and its central domain bound to NS3 (Bartenschlager et al., 1995), further stabilizing the membrane association of the NS3/NS4A complex.

Because of the importance of the NS3 amphipathic helix α_0 in the HCV life cycle, strategies to interfere with the structure and function of the helix α_0 may antagonize HCV infection. The N-terminal amphipathic α-helix AH2 of NS4B (4BAH2) was a major determinant for NS4B oligomerization, membrane association as well as NS4B-meidated aggregation of lipid vesicles, and was essential for the HCV genome replication (Gouttenoire et al., 2009a, 2010). *In vitro* screening yielded a class of small molecule inhibitors that targeted the 4BAH2 to prevent HCV replication by destroying the helix functions in oligomerization or membrane association (Cho et al., 2010). The similar strategy could be employed to screen inhibitors that either disrupt the formation of NS3 helix α_0 or impair its association with membrane. Such inhibitors could be a good addition to the current anti-HCV development many of which target the active sites of the NS3 protease.

Materials and methods

Plasmids and antibodies

pET21b-JFH1-NS3-WT was constructed by PCR amplification of a JFH1-NS3 fragment from pUC-JFH1 (Kato et al., 2003) and cloning into the NheI and XhoI sites of pET21b (Novagen, Madison, WI, USA). Plasmids pEF/JFH1-Rz/S and pEF/JFH1–GND-Rz/S constructs were kindly provided by Dr. Jake Liang (National Institutes of Health, USA). Plasmid pHA-NS2-3-WT was constructed by PCR amplification of a JFH1 NS2-3 fragment from pUC-JFH1 and cloning into the BamHI and XbaI sites of pIPHA2 (Li et al., 2007). pHA-NS2-3-

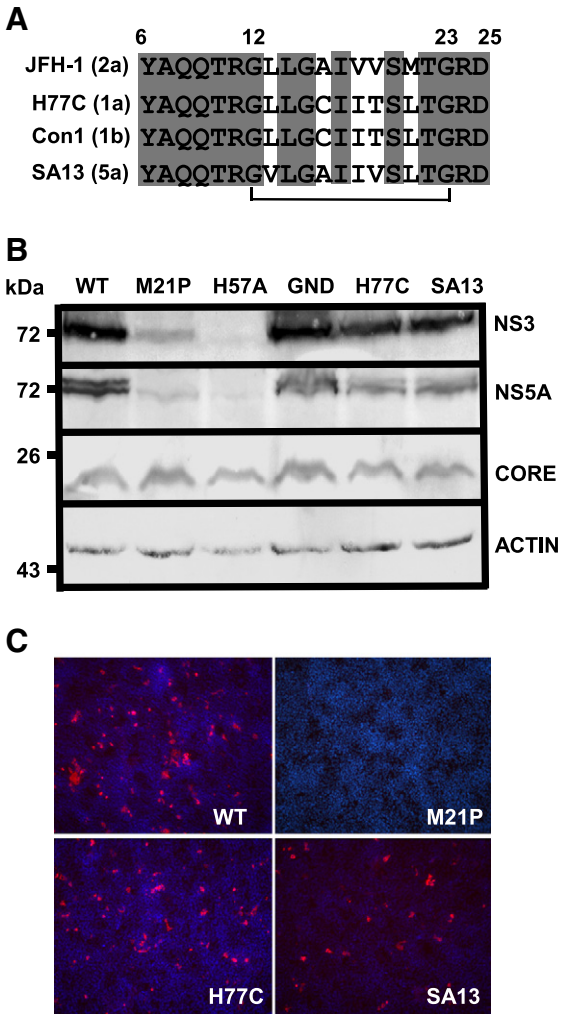

Fig. 7. NS3 stability and HCV RNA replication were restored by replacement of NS3 with the same segment from other HCV genotypes. A. Alignment of NS3 helix α_0 sequences of different HCV genotypes. Amino acids are numbered with respect to NS3 of JFH1 strain. Consensus sequences are shaded gray and the NS3 helix α_0 indicated by a line below. B. Western blot analysis of wild-type and chimeras viral proteins in the Huh7.5.1 cells transfected with the Rz plasmids expressing HCVcc, The cell lysates were collected at 48 h post transfection and examined by western blot for HCV Core, NS3 and NS5A expressions. C. Immunofluorescence of E2-positive Huh7.5.1 cells transfected with Rz-JFH1-WT and mutant/chimera constructs at 6 days post transfection. Nuclei (blue) were stained with Hoechst dye.

NS5Ahelix was constructed by recombinant fusion PCR to replace the NS3 helix α_0 fragment with the helix of NS5A. Plasmid pNS3-4A-3flag-WT was constructed by PCR amplification of a NS3-4A fragment from pUC-JFH1 and cloning into the HindIII and XbaI sites of p3XFLAG-CMV-14 (Sigma, St. Louis, MO, USA). Plasmids pNS310-24wt-GFP were constructed as described in (Brass et al., 2008). Briefly, oligonucleotides NS3-10-24wt-fwd and NS3-10-24wt-rev were hybridized and ligated into pEGFP-N1 at the XhoI and PstI sites. All point mutations were introduced using the QuikChange Site-Directed Mutagenesis Kit (Stratagene, Santa Clara, CA, USA), and verified by sequencing.

Anti-mouse monoclonal Core antibody (C7-50, Abcam, Cambridge, United Kingdom), monoclonal NS3 antibody (8G-2, Abcam), anti-rabbit polyclonal NS5A (provided by Dr. Kunitada Shimotohno, Kyoto University, Japan), monoclonal anti-Flag (M2, Sigma), anti-HA (Sigma), anti-Actin (Sigma), anti-cIAPI (provided by Dr. Hongbin Shu, Wuhan University, China), anti-Calnexin (Ab10286, Abcam), anti-human E2 antibody (C1) (Gastaminza et al., 2006) (provided by Dr. Denis Burton, The Scripps Research Institute, USA), and anti-mouse NS3 (CC3, Center for Bioengineering and Biotechnology, Henan, China) were used in the study.

Cell culture and transfection

Cell culture conditions were described previously (Zhong et al., 2006). Plasmid DNA transfection in Huh7 and Huh7.5.1 cells was performed with Lipofectamin 2000 (Invitrogen) according to the manufacturer's instructions.

In vitro transcription, HCV RNA transfection, indirect immunofluorescence, titration analysis, HCV infection kinetics assay and western blot

These procedures were as described previously (Li et al., 2010; Zhong et al., 2006).

Confocal laser scanning microscopy

The cells were washed with PBS and fixed in 4% paraformaldehyde for 30 min at room temperature. Fixed cells were washed three times with PBS and the nuclei were stained with Hoechst for 30 min at room temperature. GFP fluorescence was examined directly by confocal laser scanning microscopy (DM6000B, Leica, Germany).

Peptide synthesis and circular dichroism analysis

Peptides NS3[10–24]-WT (TRGLLGAIVVSMTGR), NS3[10–24]-M21P (TRGLLGAIVVSPTGR) were synthesized and purified to the purity of >98% by RP-HPLC (GL Biochem Ltd, Shanghai, China). Circular dichroism was performed according to the protocol described previously (Brass et al., 2008). Briefly, 45 μM of peptides were dissolved in the membrane mimic buffer 1% lysophosphatidyl choline. Circular dichroism spectra were recorded from 190 nm to 250 nm wavelength range with a 0.2-nm increment, 0.5-nm bandwidth, and one-second response time on a J700 spectrometer (J-715, JASCO, Tokyo, Japan). Spectra were baseline corrected, smoothed and processed using the JASCO program J-700.

Membrane fractionation assay

Membrane fractionation assay was performed using a cyto-mem-nucl fraction kit (Applygen Technologies Inc, Beijing, China). Briefly, ten million Huh7.5.1 cells were lysed in 0.5 ml of cytosol extraction reagent buffer and put on ice for 2 min. Lysates were douce-homogenized for 45 times, sheared by 10 passages through a 21-gage needle, and centrifugated at 800×*g* for 5 min at 4 °C. Supernatants containing the cytosol-membrane fraction were collected and mixed with 35 μl of membrane extraction reagent buffer on ice for 5 min, and then centrifugated at a maximum speed of 14000×*g* for 30 min at 4 °C. The supernatants containing the cytosolic fraction and the pellets containing the membrane fraction were collected respectively.

Membrane floatation assay

Membrane floatation assay has been described previously (Penin et al., 2004). Briefly, 2×10^7 U2-OS cells transfected with plasmids expressing the wild-type or M21P NS3-NS4A were Dounce homogenized in the hypotonic buffer (10 mM Tris–HCl, pH 7.52 mM $MgCl_2$) supplemented with complete protease inhibitor cocktail (Roche, Basel, Switzerland) followed by centrifugation at 1,000 g for 5 min to pellet nuclei and unbroken cells. Supernatant was mixed with 100% sucrose in TNE buffer (100 mM NaCl, 10 mM Tris, 1 mM EDTA, pH 7.4) to a final sucrose concentration of 73%, and placed at the bottom of a centrifuge tube. Then 65% sucrose in TNE and 10% sucrose were layered on top of the 73% sucrose successively and centrifuged at 35,000 *g* for 16 h at 4 °C. Ten fractions were collected

from the top and the distribution of NS3 proteins was analyzed by western blot.

Expression and purification of recombinant NS3 proteins

Escherichia coli Rosetta/pLysS (Novagen) containing pET21b vector expressing C-terminally 6X His-tagged NS3 protein was induced with 1 mM IPTG at 18 °C for 4 h. Cells were suspended in suspension buffer (50 mM NaH2PO4 pH 8.0, 500 mM NaCl, 0.1% Triton X-100, 0.1% 2-mercaptoethanol, 1 mM PMSF, and 2 mM imidazole) and lysed by sonication. After centrifugation at 12000 *g* for 30 min at 4 °C (Beckman JA rotor), the supernatant was incubated with Ni-NTA agarose (Qiagen), and bound NS3 proteins were eluted with elution buffer (500 mM NaCl, 20 mM Tris/HCl, pH 8.0, 0.1% Triton X-100, and 0.1% 2-mercaptoethanol, 250 mM imidazole). Proteins were loaded onto a fast performance liquid chromatography (FPLC) Superdex-200 gel filtration column equilibrated in FPLC buffer (50 mM Tris–HCl, pH 8.0, 1 mM EDTA, 10% glycerol, and 1 mM DTT, 500 mM NaCl). The purity of isolated proteins was examined by electrophoresis on a 10% SDS-polyacrylamide gel electrophoresis gel and stained with coomassie blue. Purified proteins were stored at −80 °C.

NTPase assay

A 10 μl reaction mixture was made with 50 mM Tris pH 7.0, 2 mM $MgCl_2$, 1 mM cold GTP spiked with 5 uCi [γ-^{32}P] GTP (PerkinElmer, Waltham, MA, USA), 5 pmol template and 5 pmol NS3 proteins. The reaction mixture was incubated at 37 °C for 30 min and stopped with 50 mM EDTA. One-tenth of the reaction mixture was spotted onto a thin-layer chromatography plate coated with polyethyleneimine cellulose (Sorbent Technologies, Norcross, GA, USA). Radioactive phosphate hydrolyzed from [γ-^{32}P] GTP was separated by thin-layer chromatography using 1.5 M KH_2PO_4 (pH 3.5) as a running buffer. Hydrolyzed phosphate was quantified with a PhosphorImager (Typhoon, GE Healthcare, Piscataway, NJ, USA).

Helicase assay

NS3 helicase activity was measured in a 10 μl reaction mixture containing 20 mM HEPES, pH 7.5, 2 mM dithiothreitol, 100 μg/ml bovine serum albumin, 3 mM $MgCl_2$, enzyme and substrate as indicated, and 0.5 pmol of a 30-nucleotide capture oligonucleotide (5′-TTAA-CCGCCGCCCAGGTGTGAGGA-GTACCA-3′). The reaction was initiated by addition of 5 mM ATP and incubated at 37 °C for 30 min, and stopped by addition of glycerol loading buffer containing 20 mM EDTA and 0.5% SDS. Products were analyzed in a 12% native polyacrylamide gel and quantified with a PhosphorImager (Typhoon, GE).

NS3-NS4A interaction analysis

The recombinant wild-type and M21P NS3 proteins were prepared as described above. NS4A peptide (STWVLAGGVLAAVAAYCLATGCV-SIIGRLHVNQRVVVAPDKEVLYEAFDEMEEC{K-(Bio)}KKK) was synthesized and purified by RP-HPLC (purity > 97%) with biotin labeled at its C-terminus (GL Biochem Ltd, Shanghai, China). The assay was performed with a Biacore T100 SPR biosensor instrument with 100 nM NS4A dissolved in HBS-ET buffer (50 mM HEPES, pH 7.4, 150 mM NaCl, 3 mM EDTA, 0.005% Tween 20) immobilized to the SA chip through the interaction of biotin-strepavidin at 10 μl/min for 20 s, with three repeated injections. This procedure generated surfaces of NS4A and blank. Interaction experiments were carried out at 25 °C with HBS-ET as the running buffer. Different concentrations of NS3 from 20.8 nM to 416 nM were injected as analyte to flow through the NS4A coupled surfaces at rate of 30 μl/min and with contact time of 3 min. Analysis of the sensorgrams was performed using Biacore T100 Evaluation software (GE Heathcare Life Sciences). Kinetic parameters of the interactions were determined by global analysis of at least four concentrations of the analyte using an equation representing the 1:1 binding model. The parameters of Chi^2 and U-value were included for the quality control.

Acknowledgments

We thank Dr. Francis Chisari (Scripps Research Institute, San Diego, USA) for providing Huh 7.5.1 cells, Dr. Takaji Wakita (National Institute of Infectious Diseases, Tokyo, Japan) for providing the JFH1 molecular clone, Drs. Mansun Law and Dennis Burton (Scripps Research Institute) for providing recombinant human IgG anti-E2, and Dr. Kunitada Shimotohno (Kyoto University, Kyoto, Japan) for providing anti-NS5A antibodies, Dr. Man Zhang (China Novartis Institute, Shanghai, China) for advices on Biacore analysis.

This study was supported by grants from the MOST 973 Program (2009CB522501; 2009CB522504), the National Natural Science Foundation of China (30870127), the National Key Programs on Infectious Disease (2008ZX10002-014), Chinese Academy of Science (KSCX1-YW-10), Shanghai Pasteur Health Research Foundation (SPHRF2009001) and SA-SIBS Scholarship Program.

References

Bartenschlager, R., Ahlborn-Laake, L., Mous, J., Jacobsen, H., 1993. Nonstructural protein 3 of the hepatitis C virus encodes a serine-type proteinase required for cleavage at the NS3/4 and NS4/5 junctions. J. Virol. 67 (7), 3835–3844.

Bartenschlager, R., Lohmann, V., Wilkinson, T., Koch, J.O., 1995. Complex formation between the NS3 serine-type proteinase of the hepatitis C virus and NS4A and its importance for polyprotein maturation. J. Virol. 69 (12), 7519–7528.

Brass, V., Berke, J.M., Montserret, R., Blum, H.E., Penin, F., Moradpour, D., 2008. Structural determinants for membrane association and dynamic organization of the hepatitis C virus NS3-4A complex. Proc. Natl. Acad. Sci. U. S. A. 105 (38), 14545–14550.

Cho, N.J., Dvory-Sobol, H., Lee, C., Cho, S.J., Bryson, P., Masek, M., Elazar, M., Frank, C.W., Glenn, J.S., 2010. Identification of a class of HCV inhibitors directed against the nonstructural protein NS4B. Sci. Transl. Med. 2 (15), 15ra6.

Eckart, M.R., Selby, M., Masiarz, F., Lee, C., Berger, K., Crawford, K., Kuo, C., Kuo, G., Houghton, M., Choo, Q.L., 1993. The hepatitis C virus encodes a serine protease involved in processing of the putative nonstructural proteins from the viral polyprotein precursor. Biochem. Biophys. Res. Commun. 192 (2), 399–406.

Egger, D., Wolk, B., Gosert, R., Bianchi, L., Blum, H.E., Moradpour, D., Bienz, K., 2002. Expression of hepatitis C virus proteins induces distinct membrane alterations including a candidate viral replication complex. J. Virol. 76 (12), 5974–5984.

Failla, C., Tomei, L., De Francesco, R., 1995. An amino-terminal domain of the hepatitis C virus NS3 protease is essential for interaction with NS4A. J. Virol. 69 (3), 1769–1777.

Gastaminza, P., Kapadia, S.B., Chisari, F.V., 2006. Differential biophysical properties of infectious intracellular and secreted hepatitis C virus particles. J. Virol. 80 (22), 11074–11081.

Gosert, R., Jendrsczok, W., Berke, J.M., Brass, V., Blum, H.E., Moradpour, D., 2005. Characterization of nonstructural protein membrane anchor deletion mutants expressed in the context of the hepatitis C virus polyprotein. J. Virol. 79 (12), 7911–7917.

Gouttenoire, J., Castet, V., Montserret, R., Arora, N., Raussens, V., Ruysschaert, J.M., Diesis, E., Blum, H.E., Penin, F., Moradpour, D., 2009a. Identification of a novel determinant for membrane association in hepatitis C virus nonstructural protein 4B. J. Virol. 83 (12), 6257–6268.

Gouttenoire, J., Montserret, R., Kennel, A., Penin, F., Moradpour, D., 2009b. An amphipathic alpha-helix at the C terminus of hepatitis C virus nonstructural protein 4B mediates membrane association. J. Virol. 83 (21), 11378–11384.

Gouttenoire, J., Roingeard, P., Penin, F., Moradpour, D., 2010. Amphipathic alpha-helix AH2 is a major determinant for the oligomerization of hepatitis C virus nonstructural protein 4B. J. Virol. 84 (24), 12529–12537.

Grakoui, A., McCourt, D.W., Wychowski, C., Feinstone, S.M., Rice, C.M., 1993a. Characterization of the hepatitis C virus-encoded serine proteinase: determination of proteinase-dependent polyprotein cleavage sites. J. Virol. 67 (5), 2832–2843.

Grakoui, A., McCourt, D.W., Wychowski, C., Feinstone, S.M., Rice, C.M., 1993b. A second hepatitis C virus-encoded proteinase. Proc. Natl. Acad. Sci. U. S. A. 90 (22), 10583–10587.

Hijikata, M., Kato, N., Ootsuyama, Y., Nakagawa, M., Shimotohno, K., 1991. Gene mapping of the putative structural region of the hepatitis C virus genome by in vitro processing analysis. Proc. Natl. Acad. Sci. U. S. A. 88 (13), 5547–5551.

Hijikata, M., Mizushima, H., Akagi, T., Mori, S., Kakiuchi, N., Kato, N., Tanaka, T., Kimura, K., Shimotohno, K., 1993. Two distinct proteinase activities required for the processing of a putative nonstructural precursor protein of hepatitis C virus. J. Virol. 67 (8), 4665–4675.

Kato, T., Date, T., Miyamoto, M., Furusaka, A., Tokushige, K., Mizokami, M., Wakita, T., 2003. Efficient replication of the genotype 2a hepatitis C virus subgenomic replicon. Gastroenterology 125 (6), 1808–1817.

Kato, T., Matsumura, T., Heller, T., Saito, S., Sapp, R.K., Murthy, K., Wakita, T., Liang, T.J., 2007. Production of infectious hepatitis C virus of various genotypes in cell cultures. J. Virol. 81 (9), 4405–4411.

Kim, D.W., Gwack, Y., Han, J.H., Choe, J., 1995. C-terminal domain of the hepatitis C virus NS3 protein contains an RNA helicase activity. Biochem. Biophys. Res. Commun. 215 (1), 160–166.

Kim, J.L., Morgenstern, K.A., Lin, C., Fox, T., Dwyer, M.D., Landro, J.A., Chambers, S.P., Markland, W., Lepre, C.A., O'Malley, E.T., Harbeson, S.L., Rice, C.M., Murcko, M.A., Caron, P.R., Thomson, J.A., 1996. Crystal structure of the hepatitis C virus NS3 protease domain complexed with a synthetic NS4A cofactor peptide. Cell 87 (2), 343–355.

Li, B., Samanta, A., Song, X., Iacono, K.T., Bembas, K., Tao, R., Basu, S., Riley, J.L., Hancock, W.W., Shen, Y., Saouaf, S.J., Greene, M.I., 2007. FOXP3 interactions with histone acetyltransferase and class II histone deacetylases are required for repression. Proc. Natl. Acad. Sci. U. S. A. 104 (11), 4571–4576.

Li, R., Qin, Y., He, Y., Tao, W., Zhang, N., Tsai, C., Zhou, P., Zhong, J., 2010. Production of hepatitis C virus lacking the envelope-encoding genes for single-cycle infection by providing homologous envelope proteins or vesicular stomatitis virus glycoproteins in trans. J. Virol. 85 (5), 2138–2147.

Lindenbach, B.D., Evans, M.J., Syder, A.J., Wolk, B., Tellinghuisen, T.L., Liu, C.C., Maruyama, T., Hynes, R.O., Burton, D.R., McKeating, J.A., Rice, C.M., 2005. Complete replication of hepatitis C virus in cell culture. Science 309 (5734), 623–626.

Lohmann, V., Korner, F., Herian, U., Bartenschlager, R., 1997. Biochemical properties of hepatitis C virus NS5B RNA-dependent RNA polymerase and identification of amino acid sequence motifs essential for enzymatic activity. J. Virol. 71 (11), 8416–8428.

Lohmann, V., Korner, F., Koch, J., Herian, U., Theilmann, L., Bartenschlager, R., 1999. Replication of subgenomic hepatitis C virus RNAs in a hepatoma cell line. Science 285 (5424), 110–113.

Moradpour, D., Brass, V., Gosert, R., Wolk, B., Blum, H.E., 2002. Hepatitis C: molecular virology and antiviral targets. Trends Mol. Med. 8 (10), 476–482.

Moradpour, D., Gosert, R., Egger, D., Penin, F., Blum, H.E., Bienz, K., 2003. Membrane association of hepatitis C virus nonstructural proteins and identification of the membrane alteration that harbors the viral replication complex. Antiviral Res. 60 (2), 103–109.

Munoz, V., Serrano, L., 1994. Elucidating the folding problem of helical peptides using empirical parameters. Nat. Struct. Biol. 1 (6), 399–409.

Penin, F., Brass, V., Appel, N., Ramboarina, S., Montserret, R., Ficheux, D., Blum, H.E., Bartenschlager, R., Moradpour, D., 2004. Structure and function of the membrane anchor domain of hepatitis C virus nonstructural protein 5A. J. Biol. Chem. 279 (39), 40835–40843.

Reed, K.E., Rice, C.M., 1998. Molecular characterization of hepatitis C virus. Curr. Stud. Hematol. Blood Transfus. (62), 1–37.

Satoh, S., Tanji, Y., Hijikata, M., Kimura, K., Shimotohno, K., 1995. The N-terminal region of hepatitis C virus nonstructural protein 3 (NS3) is essential for stable complex formation with NS4A. J. Virol. 69 (7), 4255–4260.

Schregel, V., Jacobi, S., Penin, F., Tautz, N., 2009. Hepatitis C virus NS2 is a protease stimulated by cofactor domains in NS3. Proc. Natl. Acad. Sci. U. S. A. 106 (13), 5342–5347.

Shimotohno, K., Tanji, Y., Hirowatari, Y., Komoda, Y., Kato, N., Hijikata, M., 1995. Processing of the hepatitis C virus precursor protein. J. Hepatol. 22 (1 Suppl.), 87–92.

Takamizawa, A., Mori, C., Fuke, I., Manabe, S., Murakami, S., Fujita, J., Onishi, E., Andoh, T., Yoshida, I., Okayama, H., 1991. Structure and organization of the hepatitis C virus genome isolated from human carriers. J. Virol. 65 (3), 1105–1113.

Tanji, Y., Hijikata, M., Satoh, S., Kaneko, T., Shimotohno, K., 1995. Hepatitis C virus-encoded nonstructural protein NS4A has versatile functions in viral protein processing. J. Virol. 69 (3), 1575–1581.

Targett-Adams, P., McLauchlan, J., 2005. Development and characterization of a transient-replication assay for the genotype 2a hepatitis C virus subgenomic replicon. J. Gen. Virol. 86 (Pt 11), 3075–3080.

Wakita, T., Pietschmann, T., Kato, T., Date, T., Miyamoto, M., Zhao, Z., Murthy, K., Habermann, A., Krausslich, H.G., Mizokami, M., Bartenschlager, R., Liang, T.J., 2005. Production of infectious hepatitis C virus in tissue culture from a cloned viral genome. Nat. Med. 11 (7), 791–796.

Zhang, C., Cai, Z., Kim, Y.C., Kumar, R., Yuan, F., Shi, P.Y., Kao, C., Luo, G., 2005. Stimulation of hepatitis C virus (HCV) nonstructural protein 3 (NS3) helicase activity by the NS3 protease domain and by HCV RNA-dependent RNA polymerase. J. Virol. 79 (14), 8687–8697.

Zhong, J., Gastaminza, P., Cheng, G., Kapadia, S., Kato, T., Burton, D.R., Wieland, S.F., Uprichard, S.L., Wakita, T., Chisari, F.V., 2005. Robust hepatitis C virus infection in vitro. Proc. Natl. Acad. Sci. U. S. A. 102 (26), 9294–9299.

Zhong, J., Gastaminza, P., Chung, J., Stamataki, Z., Isogawa, M., Cheng, G., McKeating, J.A., Chisari, F.V., 2006. Persistent hepatitis C virus infection in vitro: coevolution of virus and host. J. Virol. 80 (22), 11082–11093.